

# A VIRTUAL THERMODYNAMIC TEMPERATURE CONCEPT IN 2D OBSTACLE ENVIRONMENT FOR AUTONOMOUS MOBILE ROBOT

AKWARA, U.C  
DATA ACQUISITION ENGINEER  
(WESTERN AFRICA)WEAFRI WELL SERVICES COMPANY LIMITED  
EMAIL: uchenacha@yahoo.com, ikebull@yahoo.com, weafri@weafri.com

**ABSTRACT:** In this paper, the virtual thermodynamic temperature concept (VTTC) proposed for 2D obstacle environment for autonomous mobile robot is welcome. The concept emphasis on the heat transfer and temperature measurement of an obstacle and robot workspace with reference to the virtual target concept (VTC) for Lengthy, Concave and Wave concave shaped obstacle. This method is used to address the heat transfer (internal) and the temperature incremental area that occur in 2D workspace for autonomous mobile robot. The simulation was performed on Pentium IV Laptop, window XP (2005), 2GB Memory, 1GB Processor and 40GB Hard disk for file storage.

**KEYWORDS:** 2D, Thermodynamic, Temperature, Workspace, Calorimetric, Lengthy, Concave, Wave concave, Obstacle, Heat.

## 1. Introduction

Within this context, the virtual thermodynamic equations were used to update the internal temperature of the robot and obstacle. The 2D environment of the heat transferred by the robot primarily affects the temperature of the obstacle and send signal to the corresponding robot and target along its path. Temperature is the degree of hotness and coldness of a body in a particular environment [1] while thermodynamic is the study of motion of heat (internal and external) in a confined material medium and the process involved in the heat transfer. There are Literature updates to this approach. Farinde et al [1] reported that heat is a form of energy that can be conveyed from one body (obstacle) to another due to temperature difference while Calin [2] reported that temperature sensors are used in robotics with increasing complexity of tasks that can be done.

Nakamura and Mahrt [3] investigated the radiatively induced error in the air temperature estimate by the Onset HOBO Pro-thermistor in a naturally ventilated multiplate shield and also Tamilselvi et al [4] reported that robots are constantly faced with new situation for which there are no pre-programmed motions and planning that has to be sensor-based, implying incomplete and inaccurate world model. Huawei et al [5] investigated that there are slop and temperature distribution models in the working space of mobile robot and every node is equipped with temperature sensor and inclinometer.

Furthermore, Hillenbrand et al [6] introduce the fundamental thermodynamic equation that describes the pressure change in a control volume because of air flow through leakages or valves from or to the outside of this volume while Mataric et al [10] developed an obstacle avoidance method capable of maintaining rapid multi-robot formation through complex environment and use principles of thermodynamic in a group-level obstacle avoidance algorithm.

## 2. Problem Confirmation

This section highlights the problems for 2D obstacle, robot and target in an environment without internal temperature and thermodynamic measurement in a workspace for a Lengthy, Concave and Wave concave shaped obstacle.

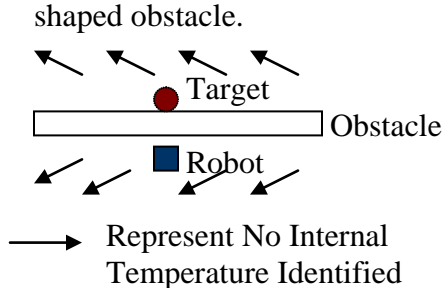


Figure 1. The diagram of Lengthy obstacle without internal temperature Identified

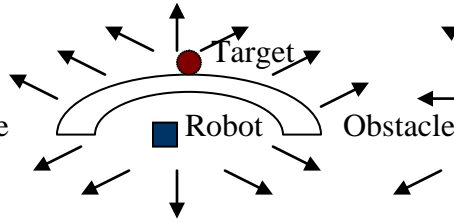


Figure 2. The diagram of Concave obstacle without internal temperature Identified

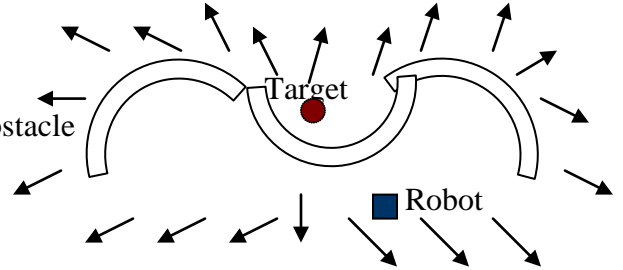


Figure 3. The diagram of Wave concave obstacle without internal temperature Identified

## 3. Solution Proposed

This section presents the virtual thermodynamic temperature(VTT) algorithm, virtual target concept (VTC) and the flow chart to solve the problem identified in section 2.

### 3.1 Virtual Thermodynamic Temperature (VTT) Algorithm

Assuming the diagram below is the environment for 2D workspace of the robot, obstacle and target placed in the histogram grid of the cell (i,j) for the virtual thermodynamic temperature to be experience.

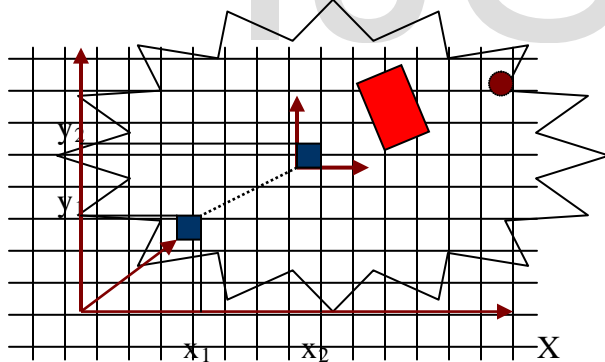
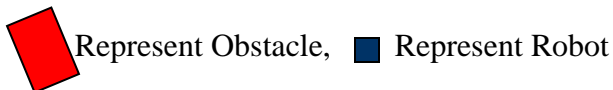
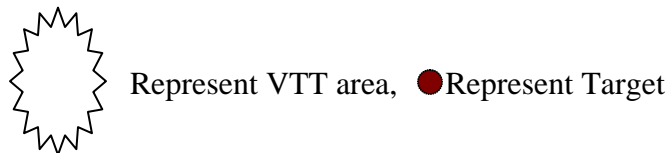


Figure 4. The sketch of VTT area surrounding a robot, Obstacle and target.



The robot is in the virtual thermodynamic workspace of cell (i,j). The thermo dynamic internal temperature measurement of the Lengthy, Concave and Wave concave shaped obstacle and robot for a calorimetric condition is given as:

$$\Delta T_{(i,j)}^n = \frac{Q_{R(i,j)}}{M_{R(i,j)} C_{R(i,j)}} \quad (1)$$

$$Q_{R(i,j)} = M_{R(i,j)} C_{R(i,j)} \Delta T_{(i,j)}^n \quad (2)$$

$Q_{R(i,j)}$  = Quantity of heat between robot and cell (i,j)

$M_{R(i,j)}$  = Mass of robot in the temperature cell (i,j).

Temperature affects the obstacle and the environment where the target and robot are placed.

$$\Delta T_{(i,j)}^n = T_{2(i,j)}^n - T_{1(i,j)}^n \quad (3)$$

$$\Delta T_{(i,j)} = T_{2(i,j)} - T_{1(i,j)} \quad (4)$$

The heat conductivity is a response of the temperature which affect the environment of the obstacle, target and robot, then

$$T_{2(i,j)} - T_{1(i,j)} = \frac{Q_{R(i,j)} d_{(i,j)}}{KA_{(i,j)}} \quad (5)$$

Where,

$d_{(i,j)}$  = Robot distance to the cell (i,j)

$A_{(i,j)}$  = Surface Area of contact to the cell (i,j)

$C_{R(i,j)}$  = Specific heat capacity of the robot to the cell (i,j)

$K$  = Conductivity proportionality constant with respect to temperature

$T_{1(i,j)}$  = Initial temperature of the environment to the cell (i,j)

$T_{2(i,j)}$  = Final temperature of the environment to the cell (i,j).

Taking the robot distance to the cell into consideration

$$d_{(i,j)} = \sqrt{(y_2 - y_1)^2_j - (x_2 - x_1)^2_i}$$

$$A_{(i,j)} = \pi r^2_{(i,j)} \quad (7)$$

Substituting equation 6 and 7 into equation 5, then

$$T_{2(i,j)} - T_{1(i,j)} = \frac{Q_{R(i,j)} \sqrt{(y_2 - y_1)^2_j - (x_2 - x_1)^2_i}}{K \pi r^2_{(i,j)}} \quad (8)$$

Making  $Q_{R(i,j)}$  the subject of the formula

$$Q_{R(i,j)} = \frac{K \pi r^2_{(i,j)} (T_{2(i,j)} - T_{1(i,j)})}{\sqrt{(y_2 - y_1)^2_j - (x_2 - x_1)^2_i}} \quad (9)$$

Substituting equation 9 into equation 1, then

$$\Delta T^n_{(i,j)} = \frac{K \pi r^2_{(i,j)} (T_{2(i,j)} - T_{1(i,j)})}{\sqrt{(y_2 - y_1)^2_j - (x_2 - x_1)^2_i}} \times \frac{1}{M_{R(i,j)} C_{R(i,j)}} \quad (10)$$

$$\Delta T^n_{(i,j)} = \frac{K \pi r^2_{(i,j)} M_{R(i,j)} C_{R(i,j)} (T_{2(i,j)} - T_{1(i,j)})}{\sqrt{(y_2 - y_1)^2_j - (x_2 - x_1)^2_i}} \quad (11)$$

$$T^n_{2(i,j)} - T^n_{1(i,j)} = \frac{K \pi r^2_{(i,j)} M_{R(i,j)} C_{R(i,j)} (T_{2(i,j)} - T_{1(i,j)})}{\sqrt{(y_2 - y_1)^2_j - (x_2 - x_1)^2_i}} \quad (12)$$

Where,  $r$  = radius of the robot to cell (i,j)

$\pi$  = pie constant (3.124)

$$T^n_{2(i,j)} = T^n_{1(i,j)} + \frac{K \pi r^2_{(i,j)} M_{R(i,j)} C_{R(i,j)} (T_{2(i,j)} - T_{1(i,j)})}{\sqrt{(y_2 - y_1)^2_j - (x_2 - x_1)^2_i}} \quad (13)$$

$T^n_{1(i,j)}$  = Incremental factor of the initial internal temperature of the cell (i,j)

$T^n_{2(i,j)}$  = Incremental factor of the final internal temperature of the cell (i,j)

## (6) 3.2 Virtual Target Concept (VTC)

This section presents the virtual target concept for Local minima recovery as stated below:

1. Create a 2D Workspace for the histogram grid of cell (i,j).
2. Update and sample the sensor to correct misreading error of the robot vision.
3. Redefine a new line of sight.
4. Select the axial procedure of the robot location from (0° to 360°).
5. Select the axial line of orientation between 1 & 2, 3 & 4, 5 & 7, 6 & 8.

## 3.3 VTTC Algorithm Procedure

This section presents the Flow chart that explain the algorithm procedure.

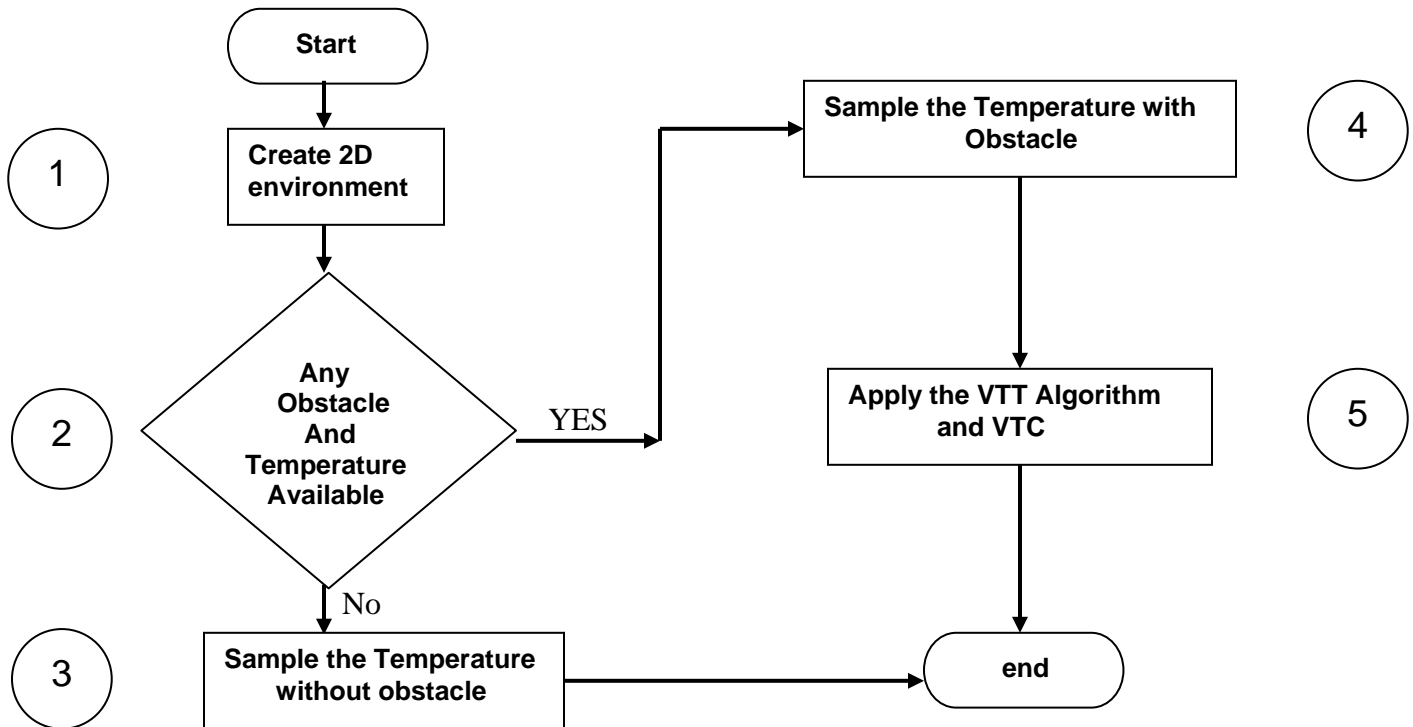


Figure 5. The Flow Chart for VTTC Algorithm Procedure

#### 4. Result and Discussion

This section presents the result and discussion obtained from the simulation. The following parameters are used in the experimental Algorithm;

$$\begin{aligned}
 Q_{R(i,j)} &= M_{R(i,j)} C_{R(i,j)} (T_{2(i,j)}^n - T_{1(i,j)}^n) \\
 &= 0.8 \times 500 \times 10.5 \\
 &= 4200J
 \end{aligned}$$

$\Pi = 3.124$ ,  $r = 0.3m$ ,  $K = 0.085Wm^{-1}K^{-1}$ ,  $M_R = 0.8kg$   
 $C_R = 500J/kg/K$ ,  $y_2 = 11$ ,  $y_1 = 3$ ,  $x_2 = 8$ ,  $x_1 = 4$ ,  
 $T_{1(i,j)} = 20^\circ C$ ,  $T_{2(i,j)} = 62^\circ C$ ,  $T_{1(i,j)}^n = (T_1 + 0.5)^\circ C$

$$\begin{aligned}
 T_{1(i,j)}^0 &= T_1 + 0.5 \\
 &= 20 + 0.5 \\
 &= 20.5^\circ C \\
 T_{1(i,j)}^1 &= T_{1(i,j)}^0 + 0.5 \\
 &= 20.5 + 0.5 \\
 &= 21^\circ C
 \end{aligned}$$

$$\begin{aligned}
 T_{1(i,j)}^2 &= T_{1(i,j)}^1 + 0.5 \\
 &= 21 + 0.5 \\
 &= 21.5^\circ C \\
 T_{1(i,j)}^3 &= T_{1(i,j)}^2 + 0.5 \\
 &= 21.5 + 0.5 \\
 &= 22^\circ C
 \end{aligned}$$

$$\begin{aligned}
 T_{2(i,j)}^0 &= T_{1(i,j)}^0 + \frac{K \Pi r^2(i,j) M_{R(i,j)} C_{R(i,j)} (T_{2(i,j)} - T_{1(i,j)})}{\sqrt{(y_2 - y_1)^2_j - (x_2 - x_1)^2_i}} \\
 &= 20.5 + \frac{0.085 \times 3.142 \times (0.3)^2 \times 500 \times (335 - 293)}{\sqrt{(11 - 3)^2 - (8 - 4)^2}} \\
 &= 20.5 + 10.5 = 31^\circ C
 \end{aligned}$$

Table 1. The Validation table for VTTC measurement and the surrounding area

S/N	T <sub>1</sub> (°C)	T <sub>2</sub> (°C)	T <sub>1</sub> <sup>n</sup> (°C)	T <sub>2</sub> <sup>n</sup> (°C)
0	20.0	62.0	20.5	31.0
1	20.0	62.0	21.0	31.5
2	20.0	62.0	21.5	32.0
3	20.0	62.0	22.0	32.5
4	20.0	62.0	22.5	33.0
5	20.0	62.0	23.0	33.5
6	20.0	62.0	23.5	34.0
7	20.0	62.0	24.0	34.5
8	20.0	62.0	24.5	35.0
9	20.0	62.0	25.0	35.5
10	20.0	62.0	25.5	36.0
11	20.0	62.0	26.0	36.5

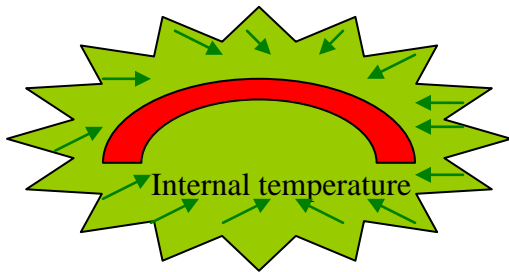


Figure 6a. The Validation clip of VTTC area surrounding an ordinary concave shaped obstacle.

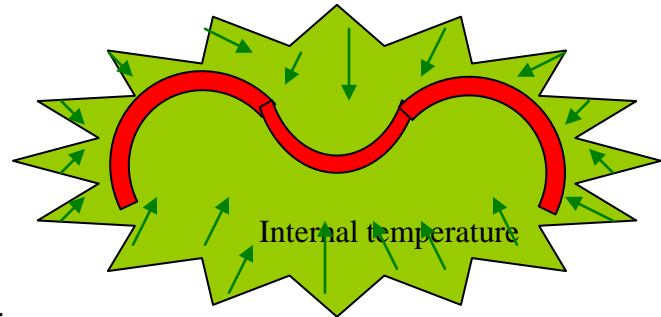


Figure 8a. The Validation clip of VTTC area Surrounding an ordinary Wave concave shaped obstacle.

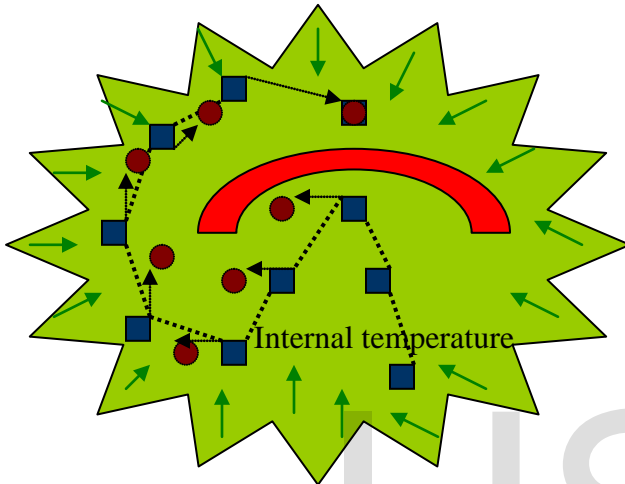


Figure 6b. The Validation clip of VTTC area Surrounding a concave shaped obstacle using VTC

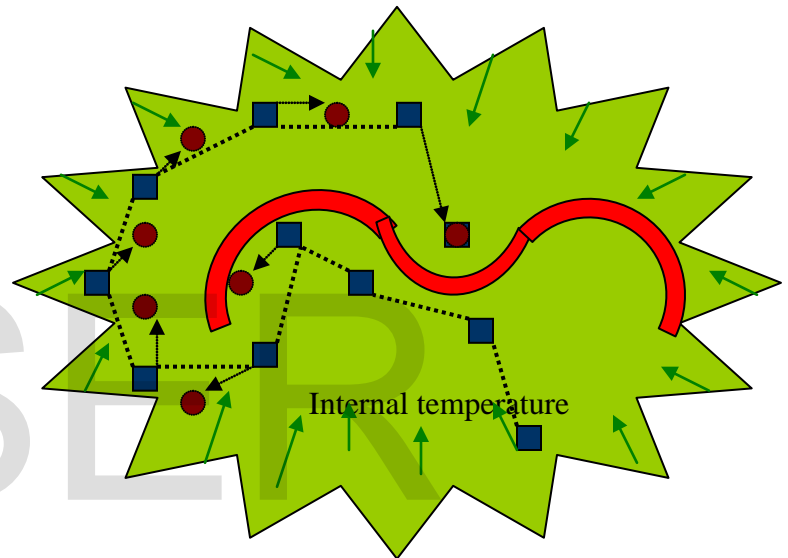


Figure 8b. The Validation clip of VTTC area surrounding a Wave concave shaped Obstacle using VTC.

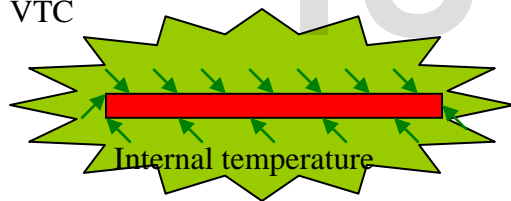


Figure 7a. The Validation clip of VTTC area Surrounding an ordinary Lengthy shaped obstacle.

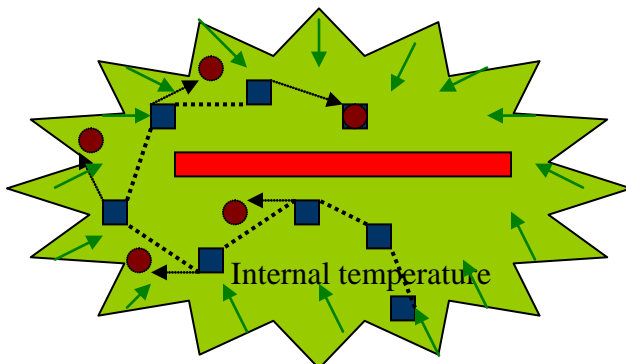


Figure 7b. The Validation clip of VTTC area Surrounding a Lengthy shaped obstacle using VTC



Represent Obstacles

● Represent Target

■ Represent Captured Target

■ Represent Mobile Robot

→ Represent Direction of internal temperature

→ Represent Direction of Virtual target

..... Represent Direction of Robot trajectory



Represent V TTC surrounding area

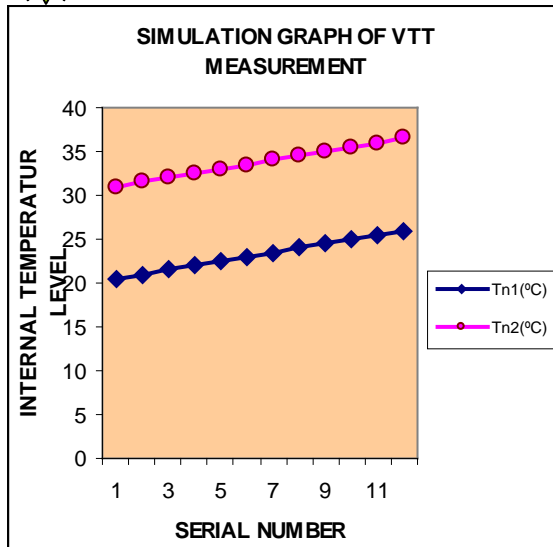


Figure 9. The Simulation Line graph of VTT measurement.

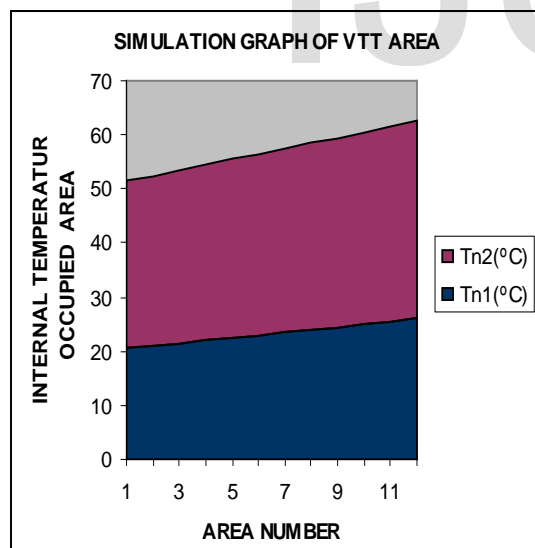


Figure 10. The Simulation Area graph of VTT occupied level.

Figure 6a. Show the Validation clip of V TTC area surrounding an ordinary concave shaped obstacle. The V TTC area is closer and the internal temperature direction is also closer to the obstacle while Figure 6b. Represent the Validation clip of V TTC area surrounding a concave shaped obstacle using VTC. The Local minima recovery is performed and the V TTC area is wider and the internal temperature direction is far apart from the obstacle.

Figure 7a. Show the Validation clip of V TTC area Surrounding an ordinary Lengthy shaped obstacle. The V TTC area is smaller and the internal temperature direction is on the obstacle and also Figure 7b. Represent the Validation clip of V TTC area surrounding a Lengthy shaped obstacle using VTC. The Local minima recovery is applied and the V TTC area is medium in size and the internal temperature direction is further apart from the obstacle.

Furthermore, Figure 8a. Show the Validation clip of V TTC area surrounding an ordinary Wave concave shaped obstacle. The V TTC area is larger and the internal temperature direction is far apart from the obstacle while Figure 8b. Represent the Validation clip of V TTC area surrounding a Wave concave shaped obstacle using VTC. The Local minima recovery is applied and the V TTC area is more wider and the internal temperature direction is much far apart from the obstacle.

Figure 9. Represent the Simulation Line graph of VTT measurement. In the graph, the smallest  $T_{1(i,j)}^n$  is 20.5(°c) and the largest value is 25.5(°c) also in the graph, the smallest  $T_{2(i,j)}^n$  is 31.0(°c) and the largest value is 36.0(°c)

Finally, Figure 10. Show the Simulation Area graph of VTT occupied level. In the graph, the blue location is the internal temperature occupied area of  $T_{1(i,j)}^n$  also in the graph, the pink location is the internal temperature occupied area of the  $T_{2(i,j)}^n$ .

Table 1. Represent the validation table for V TTC measurement and the surrounding area. The  $T_{1(i,j)}^n$  increases by 0.5(°c) while the  $T_{2(i,j)}^n$  increases by 10.5(°c) to every one  $T_{1(i,j)}^n$  at the obstacle, robot and target stage.

## Conclusion

We have practically proved from our simulation that virtual thermodynamic temperature concept (VTTC) is better, robust, efficient and simplified to the mode of heat transfer, internal temperature measurement, and VTC and Algorithm simulation. The result proved the overall performance of the internal temperature and simulation that lie in the 2D environment of the obstacle, robot and target for a Lengthy, Concave and Wave concave shaped obstacle. The future papers expected include VTT in 3D workspace for mobile robot, built prototype implementation and generalized model for thermodynamic temperature adaptation.

## Reference

- [1] Farinde et al., Essential physics, Tonad publishers ltd, 2<sup>nd</sup> edition, [www.tonadpub.com](http://www.tonadpub.com), August 2008.
- [2] Calin, Temperature sensors for robot, Smashing Robots (powered by robots), November 8, 2011.
- [3] Nakamura, R., Mahrt, L., Air temperature measurement errors in naturally ventilated radiation shields, Journal of Atmospheric and Oceanic Technology, Vol. 22, pp. 1046-1058, 2005.
- [4] Tamilselvi et al., Hybrid Approach for global path selection and dynamic obstacle avoidance for mobile robot navigation, College of Engineering, South India, Vol. 6, pp.120-132, 2010.
- [5] Huawei et al., A WSNs-based Approach and System for mobile robot navigation, Chinese Academy of science, Vol.23, pp.446-466, China.
- [6] Hillenbrand et al., Simulation of climbing robots using underpressure for Adhesion, Robotics Research Lab, pp.1-8, Germany.
- [7] Hillenbrand, C., Berns, K., A Climbing robot based on underpressure adhesion for the inspection of concrete walls. In 35<sup>th</sup> International symposium on Robotics (ISR), Paris/ France, pp.119, 2004.
- [8] Holman, J.P., Heat transfer, 10<sup>th</sup> ed, New York: McGraw-Hill, pp.27-60, 2009, Print.
- [9] Spears, W., Distributed, Physics-based control of swarms of vehicles, Autonomous Robot, Vol.7, pp. 137-162, 2004.
- [10] Mataric et al., A distributed thermodynamics- inspired Approach to Multi-Robot obstacle Avoidance, the interaction Lab, University of Southern California.
- [11] Fukuda, T., Tar, T.J., Energy, Environment and Safety issues in Robotic and Automation, IEEE Robotics and Automation's, [www.isr.uc.pt/IEEE/RAS/EES.2009](http://www.isr.uc.pt/IEEE/RAS/EES.2009).
- [12] Changqing et al., Virtual obstacle concept for Local minima recovery in PFM. Proceed of IEEE International Conference on Robotics and Automation, pp. 983-988, 2000.
- [13] Olunloyo, V.O.S., Ayomoh, M.K.O., A Path planning mode for an Autonomous vehicle in an unstructured obstacle Domain, Proceeding of the 14<sup>th</sup> IASTED International Conference, Robotics and Automations, 2009.
- [14] Bernoulli's Law.<http://scienceworld.wolfram.com/Physics/Bernoullislaw.html>.2004.